Memoirs of the Faculty of Engineering, Okayama University, Vol. 34, No. 1,2, pp.1-12, March 2000

Falling Snow Melting Characteristics of Warm Water Flowing along Sheet Channels Spread on a Roof

Baoyin SONG*, Hideo INABA**, Akihiko HORIBE** and Takashi TAKAHASHI***

(Received December 24, 1999)

The experiment for investigating the falling snow melting characteristics of warm water flowing along sheet channels spread on a roof was performed in Tookamachi city, Nigata prefecture from February 6 to February 7, 1995. The sheet surface temperatures at 11 positions in 3 channels were measured. A physical model for a gas-water-snow system was constructed to compare the predicted results with the measured ones. A fully spread uniform water film in the sheet channel was observed in the experiments. The experimental results elucidated that it was feasible to use warm water flowing along sheet channels for melting falling snow on roofs. The temperature drop in the sheet channel mainly depended on the snowfall intensity, atmospheric temperature and wind speed. Under the influence of the roof edge, the temperature drop in the channel next to the side edge was much larger than that in middle channels. A water-snow two phase flow or a snow covered frozen water was experienced temporarily in the lower reaches of the water flowing channel. These suggest that a larger water flow rate is needed for the channel next to the roof edge, and a higher inlet temperature or a greater water flow rate is required for a severe weather condition. There was reasonably good agreement between the measured and predicted water temperatures.

NOMENCLATURE

c	mass fraction of water vapor	L	roof length [m]
c_p	specific heat [J kg^{-1} K^{-1}]	m	water evaporation rate [kg s^{-1}m^{-2}] or snow-fall intensity [kg s^{-1}m^{-2}] or [mm h^{-1}]
D	mass diffusivity [m^2 s^{-1}]	M	molar mass [kg kmol^{-1}]
g	gravitational acceleration [m s^{-2}]	p	pressure [Pa]
h_{fg}	latent heat [J kg^{-1}]	q^o	solar incident radiation [W m^{-2}]
k	molecular thermal conductivity [W m^{-1} K^{-1}]		

* Department of Mechanical Engineering

** Graduate School of Natural Science and Technology

*** Patedision Co. Ltd., Ach 1-14-16, Kurashiki 710-0055

Re_l	water film Reynolds number
s	snow fraction
T	temperature [K] or [℃]
u, v	x-direction and y-direction velocities [m s^{-1}]
x, y	coordinates in axial and transverse directions [m]

Greek symbols

ρ	density [kg m^{-3}]
δ_l	water film thickness [m]
δ_g	thickness of velocity boundary layer of gas [m]
δ_r	thickness of the roof and sheet [m]
μ	dynamic viscosity [kg m^{-1} s^{-1}]
ν	kinematic viscosity [m^2 s^{-1}]
ϕ	relative humidity [%]
ψ	roof inclination [°]

Subscripts

a	of dry air
e	refers to evaporation
f	refers to fusion
g	of gas mixture of dry air and water vapor
i	condition at the gas-water interface
in	condition at the inlet
l	of liquid water
out	condition at the outlet
r	of the roof and sheet
s	of snow
v	of vapor
wb	refers to wet bulb
∞	refers to atmosphere

1. INTRODUCTION

Snow is a familiar substance in all parts of the cold regions. It presents one of the most severe hazards of a cold climate in terms of transportation and daily operations in populated areas. The accumulation of snow makes the holding substrates bear more burden or even be broken. Some measures have been used in removing or melting snow, which includes removing snow with special vehicles, road and roof heating using electrical wires, melting snow with underground or warm water, and etc.[1-2]. Tsukidate et al.[3] developed a combined system for melting snow in winter and supplying solar heated water in other seasons.

Removing snow on roofs using warm water can be divided as two ways, i. e., melting accumulated snow and falling snow. Melting accumulated snow tries to remove snow which has been already piled on the roof for a certain thickness of layer. While melting falling snow is thawing the snow with warm water as it is falling so that this prevents snow building up on the roof. However it is difficult to form a very thin uniform water film on tiles or a wide flat roof, which limits both ways mentioned above to be applied widely. For the sake of saving energy and water resource, this problem should be solved.

The present experiment makes an approach to using the special sheet channels spread on an inclined roof to form uniform water films for melting falling snow. The experiment was conducted in Tookamachi, Nigata prefecture from February 6 to February 7, 1995. The sheet surface temperatures at 11 positions in 3 channels were measured. The falling snow melting characteristics of the present system were discussed based on the experimental data and model analysis.

2. APPARATUS AND PROCEDURE

A temporal southwest facing house used for the present experiment was built in Tookamachi city, Nigata

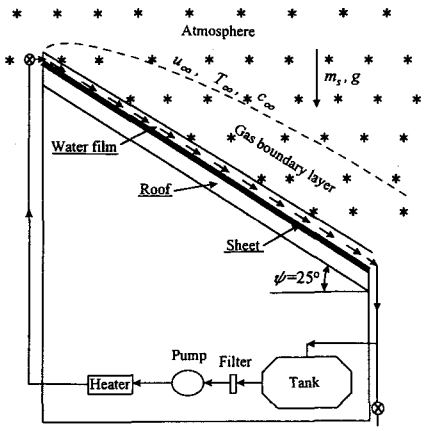

Fig. 1(a). Schematic of the experimental system

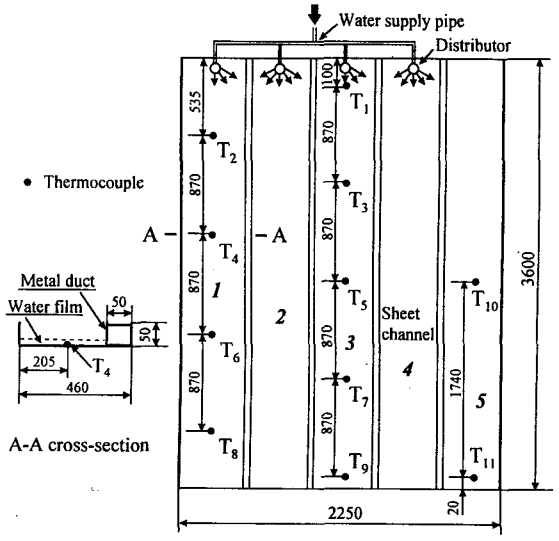

Fig. 1(b). Sheet channels and measuring positions

prefecture. The experimental system and measuring positions are illustrated in Figs. 1(a)–1(b). The roof with an inclination of 25 degree from the horizontal is 3.6 m in length. A total of 5 sheet channels with 2.25 m in width was spread on the roof from its left edge. The width of the channel is 0.41 m. The metal ducts measured 50 × 50 mm in section dimension with the wall thickness of 1.5 mm and a shallow slot of 5 mm in deep on top were stuck on the sheet as the channel walls. The 2 mm thick sheet is made of rubber-fabric with micro column stripes on its front surface to spread uniform water film flow, prevent leaking and reduce the heat loss to the roof. The roof is made of the wood plate of 18 mm in thickness. Four of the five channels are fed with water at their top end as the experiment is performed. A total of 11 thermocouples was attached to the front surfaces of three channels to measure temperatures. The thermocouples are located at the central column lines with the distance of 0.87 m between two neighboring positions in the same channel except Channel 5, in which the distance of T_{10} and T_{11} is two times larger than that in other channels. The ambient atmospheric temperature was measured with the same kind of thermocouples mentioned above, which are calibrated using a constant temperature bath with an accuracy of ± 0.1 ℃. The outputs of the thermocouples were read with a programmable automatic scanning 20-channel data logger with a printer. The collecting tank, the filter, the pump, the heater, the valves, the sheet channels and their measuring subsystem, the recycle water, and the weather conditions including snowfall intensity, m_s, atmospheric temperature, T_∞, atmospheric relative humidity, ϕ, wind speed, u_∞, and the insolation, q^o, form the experimental system. The data on snowfall intensity, atmospheric relative humidity and wind speed were obtained from Tookamachi fire station. The solar radiation was not measured as the experiment was done on the most cloudy weather condition. The volumetric flow rate of the water film in each sheet channel was determined by 500 ml graduated cylinder and a electronic watch with 0.01 second resolution.

the inlet water temperature was controlled by adjustment of a transformer which can supply power to the heater, and the initial flow rate of the water film was controlled by adjusting the valves. The house and the sheet channels on its roof snapped off are shown in Fig. 1(c). What needs to be clarified is that of the 8 channels, only five from left are used in the present experiment. Figure 1(c) shows that the roof together with its sheet channel walls is fixed with many metal frames and almost not sealed to atmosphere, which causes an unnecessary heat loss.

During the test running, filtered and heated water is pumped to the ridge of the roof. Then the water is distributed uniformly to four sheet channels. By the action of gravity, the water falls down the tilted channel as a thin film. At the bottom end of the sheet channels, the water is collected in a gutter and mostly conducted into the storage tank. The falling snow is immediately melted in the four water flowing channels in most cases, and builds up a certain thickness of snow layer in Channel 5. The measured data are scanned by the data logger every half an hour, printed out and/or sent to a personal computer to be stored or further processed.

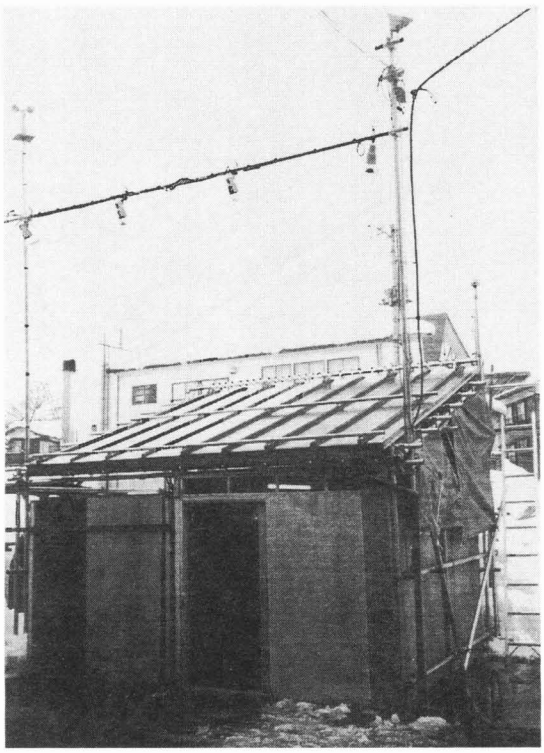

Fig. 1(c). The experimental house and the sheet channels on its roof

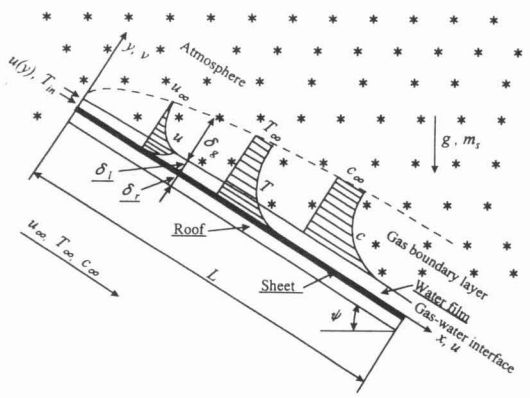

Fig. 2. Physical model and coordinate system for a gas-water-snow system

3. ANALYSIS

To support the experimental work, a mathematical model of the physical system was constructed. The thermodynamic and transport properties are functions of temperature and mixture composition. The snow temperature, T_s, was assumed to be equal to the wet bulb temperature of the atmosphere, T_{wb}, for $T_{wb} < 0$ ℃ or 0 ℃ for $T_{wb} \geq 0$ ℃. The temperature of the rain fraction was assumed to be always the same as T_{wb}. For the water flow rate of 0.029 kg/(s m) ($\mathrm{Re}_l = 90$) and the maximum wind speed of 5 m/s, a contact pattern of laminar gas – laminar water was chosen for the analysis. It was also assumed that the flow is steady two-dimensional Newtonian boundary layer flow. The physical model and coordinate system are illustrated in Fig. 2. The warm water flows downwards along the sheet channel as a thin film due to the action of gravity. By the actions of viscous and inertial forces, the stagnant ambient atmosphere or the co-current wind will flow along with the

water film forming an accompanying gas boundary layer. The snow falling on the free surface of the water film is assumed to be immediately melted. The heat is transferred by convection in the water film. The snow falling and water evaporation cause heat and mass transfer to take place simultaneously at the gas-water interface and in the gas layer. The mass transport and the velocity variation result in that the water film thickness varies along the flow direction. Heat transfer across the sheet and roof thickness is only in the form of conduction.

3.1 Governing Equations

The conservation equations for the water film are

mass

$$\frac{\partial u_l}{\partial x} + \frac{\partial v_l}{\partial y} = 0 \tag{1}$$

momentum

$$u_l \frac{\partial u_l}{\partial x} + v_l \frac{\partial u_l}{\partial y} = \frac{\partial}{\partial y}\left(\nu_l \frac{\partial u_l}{\partial y}\right) + g \sin\psi \tag{2}$$

and energy

$$\rho_l c_{p,l} u_l \frac{\partial T_l}{\partial x} + \rho_l c_{p,l} v_l \frac{\partial T_l}{\partial y} = \frac{\partial}{\partial y}\left(k_l \frac{\partial T_l}{\partial y}\right) \tag{3}$$

Neglecting the disturbance of falling snow to the gas stream, then the equations of mass, momentum, energy and concentration in the gas layer can be induced as

$$\frac{\partial(\rho_g u_g)}{\partial x} + \frac{\partial(\rho_g v_g)}{\partial y} = 0 \tag{4}$$

$$\rho_g u_g \frac{\partial u_g}{\partial x} + \rho_g v_g \frac{\partial u_g}{\partial y} = \frac{\partial}{\partial y}\left(\mu_g \frac{\partial u_g}{\partial y}\right) + g\left(\rho_g - \rho_\infty\right)\sin\psi \tag{5}$$

$$\rho_g c_{p,g} u_g \frac{\partial T_g}{\partial x} + \rho_g c_{p,g} v_g \frac{\partial T_g}{\partial y} = \frac{\partial}{\partial y}\left(k_g \frac{\partial T_g}{\partial y}\right) + \rho_g D(c_{p,v} - c_{p,a}) \frac{\partial c}{\partial y}\frac{\partial T_g}{\partial y} \tag{6}$$

and

$$\rho_g u_g \frac{\partial c}{\partial x} + \rho_g v_g \frac{\partial c}{\partial y} = \frac{\partial}{\partial y}\left(\rho_g D \frac{\partial c}{\partial y}\right) \tag{7}$$

3.2 Boundary and Interfacial Conditions

The inlet water velocity distribution was prescribed as the case for the fully developed flow without interfacial shear. To include the heat loss due to the fact of the "open" roof, the metal channel walls and the fixing metal frames, we simply assume in the analysis that the temperature at the back surface of the wooden roof is at the same value as the atmospheric temperature. Then the boundary conditions for the gas-water-snow system are

$$x = 0 \;:\quad u_l(y) = \frac{\rho_l g \sin\psi \delta_l^2}{\mu_l}\left[\frac{y}{\delta_l} - \frac{1}{2}\left(\frac{y}{\delta_l}\right)^2\right],\quad T_l = T_{in},\quad u_g = u_\infty,\quad T_g = T_\infty,\quad c = c_\infty \tag{8}$$

$$y = 0 \;:\quad u_l = 0,\quad k_l \frac{\partial T_l}{\partial y} = k_r \frac{T_l(0) - T_\infty}{\delta_r} \tag{9}$$

and

$$y \to \infty \;:\quad u_g = u_\infty,\quad T_g = T_\infty,\quad c = c_\infty \tag{10}$$

δ_r and k_r in Eq. (9) denote the thickness, and the thermal conductivity of the roof and sheet, respectively.

At the gas-water interface (y=δ_l), the continuities of velocity, temperature, mass and shear stress, and the energy balance must be met. The difference between the snowfall and the water evaporation is the main source for increasing water film thickness. As the falling snow is melted by the water film and reaches the interfacial temperature, it must receive the sensible heat that increases its temperature from T_s to 273.15 K in solid phase as well as from 273.15 K to interfacial temperature in liquid phase, and the latent heat that fuses it to water. For the rain fraction, only needed is the sensible heat in liquid phase to raise its temperature to the interfacial value. Based on the above consideration, the interfacial conditions can be

$$u_i = u_l = u_g \tag{11}$$

$$T_i = T_l = T_g \tag{12}$$

$$\rho u_i \frac{\partial \delta_l}{\partial x} = \left[\left(\frac{\partial \delta_l}{\partial x}\right)^2 + 1\right]^{1/2} (m_s \cos\psi - m_e) + \rho_{l,i} v_{l,i} \tag{13}$$

$$\left(\mu_l \frac{\partial u_l}{\partial y}\right)_{l,i} = \left(\mu_g \frac{\partial u_g}{\partial y}\right)_{g,i} \tag{14}$$

and

$$\begin{aligned} -\left(k_l \tfrac{\partial T_l}{\partial y}\right)_{l,i} &= h_{fg,e} m_e + m_s s \cos\psi [h_{fg,f} + c_{p,l}(T_i - 273.15) + c_{p,s}(273.15 - T_s)] \\ &+ m_s (1-s)\cos\psi c_{p,l}(T_i - T_{wb}) - \left(k_g \tfrac{\partial T_g}{\partial y}\right)_{g,i} \end{aligned} \tag{15}$$

By considering the solubility of air in the water film to be negligibly small, the transverse velocity of the air-vapor mixture in the gas-water interface can be

$$v_{g,i} = -\left(\frac{D}{1-c}\frac{\partial c}{\partial y}\right)_{g,i} \tag{16}$$

and the mass flux from the water film to the gas layer reads

$$m_e = \rho_{g,i} v_{g,i} \tag{17}$$

Assuming the gas-water interface at saturation pressure, $p_{v,i}$, the interfacial mass fraction of water vapor can be evaluated by

$$c_i = \frac{p_{v,i}}{(p_\infty - p_{v,i})\frac{M_a}{M_v} + p_{v,i}} \tag{18}$$

where M_a and M_v denote the molar mass of dry air and vapor, respectively.

3.3 Solution Method

A control-volume finite-difference procedure[4] was used to solve the coupled equations. A fully implicit numerical scheme was employed. In order to obtain accurate solution, the convective term is approximated by a power-law. A total of 180×224 grid points was used across the water film and gas layer thickness. The axial grid line at the gas-water interface was always located at the free surface of the water film. The system of algebraic discretization equations obtained for water and gas regions was solved through the line-by-line application of the tri-diagonal matrix algorithm. At the gas-water interface the matching discretization equations were set up by making the continuities of mass, shear stress and temperature as well as energy balances. To avoid the divergence of iterations, the time interval in the discretization equations for unsteady problems was chosen as a

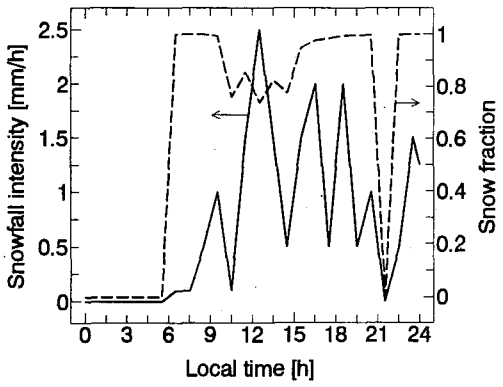

Fig. 3(a). Diurnal Changes of snowfall intensity and snow fraction on Feb. 6, 1995

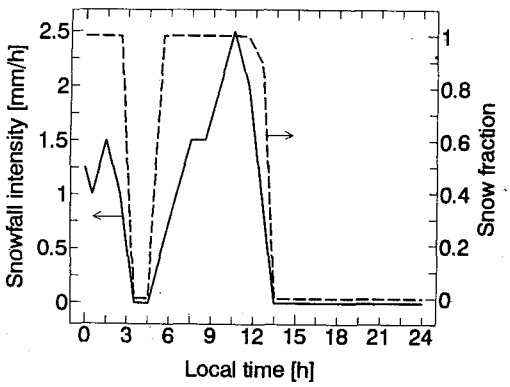

Fig. 3(b). Diurnal Changes of snowfall intensity and snow fraction on Feb. 7, 1995

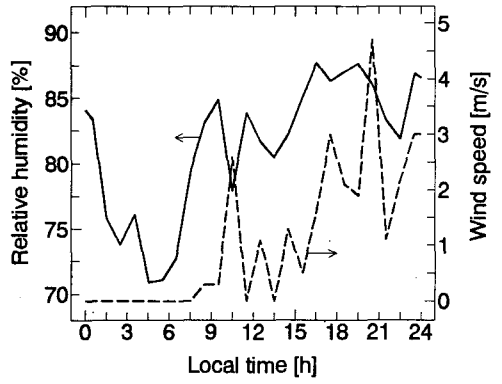

Fig. 4(a). Diurnal changes of relative humidity and wind speed on Feb. 6, 1995

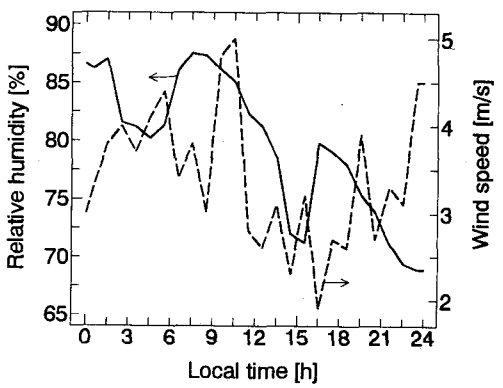

Fig. 4(b). Diurnal changes of relative humidity and wind speed on Feb. 7, 1995

specific under-relaxation factor together with another normal under-relaxation factor to solve the present steady problem.

4. RESULTS AND DISCUSSION

4.1 Experimental Conditions and Measurements

The experiment was continuously conducted in Tookamachi, Nigata prefecture for 48 hours from Feb. 6 to Feb. 7, 1995. The inlet water temperature was controlled at about 9–11 ℃, and the initial water flow rate for each of the four flowing channels was same at a value of 12 ml/s.

The weather conditions gained from Tookamachi fire station are shown in Figs. 3(a)–4(b). The snow fraction in Figs. 3(a)–3(b) was calculated by[5]

$$T_{wb} < 1.1\,℃ \quad : \quad s(T_{wb}) = 1 - 0.5\exp[(-2.2(1.1 - T_{wb})^{1.3}] \tag{19}$$

$$T_{wb} \geq 1.1\,℃ \quad : \quad s(T_{wb}) = 0.5\exp[(-2.2(1.1 - T_{wb})^{1.3}] \tag{20}$$

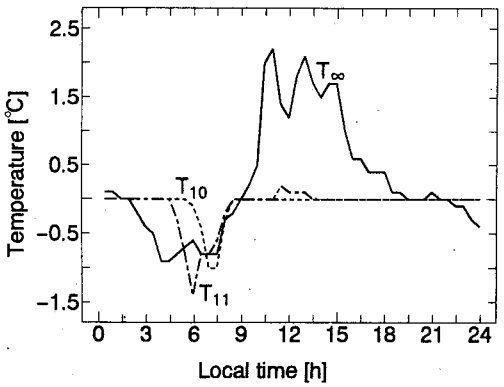

Fig. 5(a). Diurnal Changes of atmospheric tmperature and the surface temperatures in Channel 5 on Feb. 6, 1995

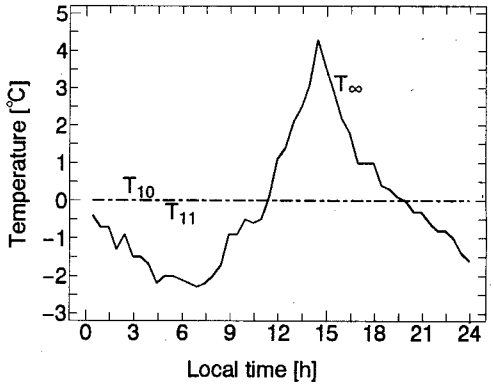

Fig. 5(b). Diurnal Changes of atmospheric tmperature and the surface temperatures in Channel 5 on Feb. 7, 1995

where T_{wb} in Celsius is atmospheric wet bulb temperature. It can be expressed approximately as

$$T_{wb} = 0.584T_a + 0.875p_v - 5.32 \tag{21}$$

In Eq. (21), T_a in Celsius is atmospheric temperature, and p_v is the water vapor pressure in atmosphere. The vapor pressure was calculated from[6]

$$p_v = \phi p_{vs} = 6.11213\phi \exp\left(\frac{17.5043T_a}{241.2 + T_a}\right) \tag{22}$$

where ϕ denotes relative humidity, and p_{vs} denotes saturation vapor pressure. Due to the higher atmospheric temperature in day time, the precipitation is not only as the form of snow. The data in Fig. 3(a) indicate that the snow fraction from 10 to 15 o' clock is around 80 % of the total precipitation, which means that the falling substance is a mixture of snow and rain. By comparing the variation of snowfall intensity in Figs. 3(a) and 3(b) with the change of relative humidity in Figs. 4(a) and 4(b), it is found that during snow falling the relative humidity generally shows a higher percentage of $\phi > 80\%$. The wind directions are mostly from south, south-southwest, and/or south-southeast. Since only a difference over 0.5 mm in the rain gauge can be identified, a value less than 0.5 mm/h for snowfall intensity is shown as 0 mm/h in the rain gauge. In addition, the windy weather made the error bigger. Therefore measured snowfall intensity would be less somewhat than its real value. The total precipitation for the two days was measured as 32 mm in water (16.5 mm on Feb. 6 and 15.5 mm on Feb. 7), which means that a snow layer of 29 cm in thickness was packed on the channel 5 based on the snow density at 100 kg/m^3 and the roof inclination of $\psi = 25°$.

Figures 5(a)–5(b) present the diurnal changes of T_{10}, T_{11} and ambient atmospheric temperature, T_∞, on Feb. 6 and Feb. 7, respectively. Under the influence of Channel 4 in which warm water was flowing as a thin film, T_{10} and T_{11} in Fig. 5(a) keeps 0 Celsius before 4 o'clock. The continuous heat loss to atmosphere made T_{11} drop from 4:30. The drop of the upper temperature, T_{10}, was delayed for 1 hour. This is attributed to that there is a temperature gradient along flow direction in the neighboring channel. From 5 o'clock, snow started to fall, and the sheet got wet, which caused T_{10} and T_{11} to drop to a value closed to the wet bulb temperature. With

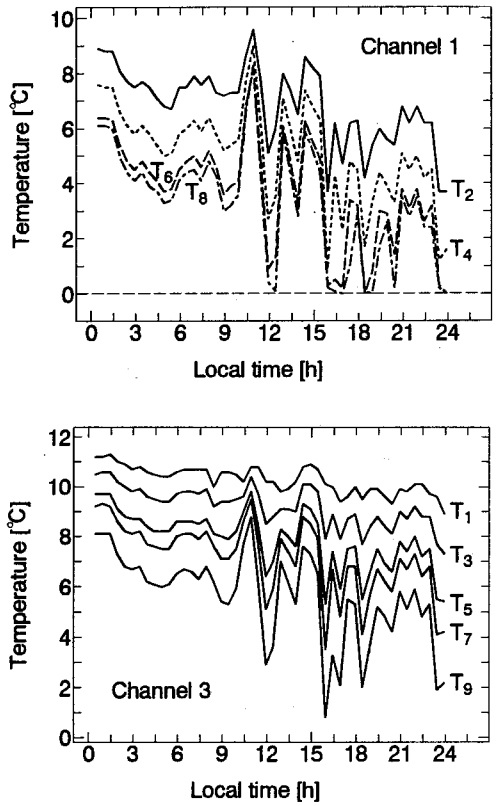

Fig. 6(a). Diurnal Changes of the surface temperatures in the two water flowing channes on Feb. 6, 1995

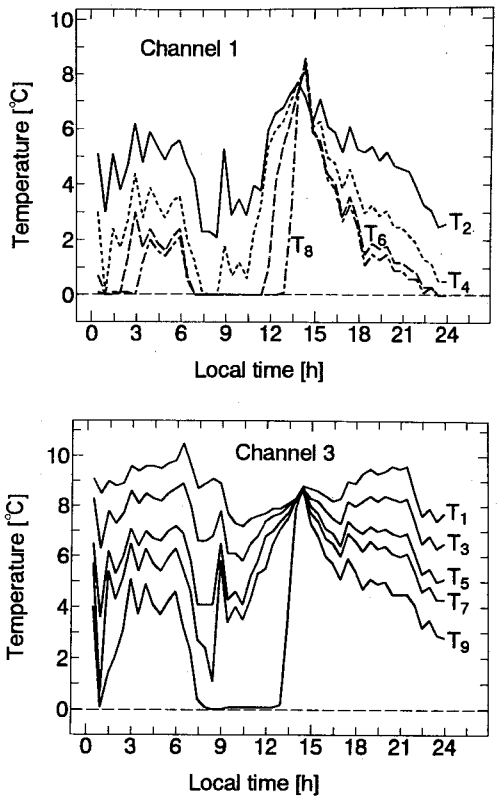

Fig. 6(b). Diurnal Changes of the surface temperatures in the two water flowing channes on Feb. 7, 1995

snow layer getting thick, the heat loss from the sheet channel to atmosphere became less so that T_{10} and T_{11} rose to 0 Celsius again. Later a micro layer of snow-water mixture formed near the sheet surface remained the channel temperature almost constant except that T_{11} was somewhat larger than 0 Celsius from 11:00 to 13:30 due to the effects of ambient temperature, a small quantity of diffuse radiation, and the fixing frame near the eaves. The state that the sheet surface temperatures in Channel 5 without water flowing over kept at ice point was extended to the end of the next day even if the snow stopped falling at 14 o'clock (see Fig. 5(b)).

The diurnal changes of the sheet surface temperatures in Channels 1 and 3 with water falling down are shown in Figs 6(a) and 6(b) for Feb. 6 and Feb. 7, respectively. By contrast with Figs. 3(a)–3(b) and 5(a)–5(b), it is found that the temperature variations are mainly influenced by the snowfall intensity and atmospheric temperature. In case of no snow falling, the temperature drop through the whole length of Channel 3 from 0:30 to 7:30 on Feb. 6 is around 3 to 4.5 ℃ (see Fig. 6(a)), and the temperature drop gets somewhat greater from 3:00 to 5:30 and from 18:30 to 24:00 on Feb. 7 for a colder and windy weather condition (reference to Figs. 6(b) and 4(b)). The large magnitude of water temperature drop in case of no snow falling is mainly attributed to the unsealed roof, the metal channel walls and its fixing frames, which play the role of fins. The temperature drop in Channel 3 is closed to 0 ℃ at 14:25 Feb. 7, which should be attributed to that the heat loss to the atmosphere was balanced by the solar radiation. The largest snowfall intensity around 12 o'clock on Feb. 6

has not resulted in a largest temperature drop, which might be attributed to a lower snow fraction (s = 0.738) and a higher wet bulb temperature (T_{wb} = 0.71 ℃). Due to the cold edge influence and/or the gathered snow intruding, the temperature drop in Channel 1 is much larger than that in Channel 3. On Feb. 6, the prevention of snow accumulating on roofs using falling warm water is successful even though a very thin layer of snow sometimes covers a distance less than 1 m from the outlet of the water flow in Channel 1 after 12 o'clock. However on Feb. 7, T_9 in Channel 3, and T_8, T_6 and T_4 in Channel 1 remain at a temperature around 0 Celsius for different time, respectively, which means that the flow beyond the sensor position becomes snow-water two phase flow or freezes up. If a heavier snow continuously falls, the melting of falling snow by the flowing water film at the flow rate and the inlet temperature given in the present experiment will be failed. The highest T_8 at 14:25 Feb. 7 is also attributed to the solar radiation and the edge influence. It is noted that the snowfall intensity was gained through the observation once an hour so that the value for snowfall intensity presented in Figs. 3(a) and 3(b) is just the average. The temperatures in Figs. 6(a) and 6(b) however were scanned every half an hour. Therefore some differences in local time corresponding to the local peak snowfall intensity and the local valley temperatures were found. The larger snowfall intensity and lower atmospheric temperature which lasted for a longer period are the main reason why the falling snow can not be totally melt in some time on Feb. 7. The differences in temperature drop between two neighboring measuring positions are mainly attributed to the influences of the fixing frames and the mounting deviation of the thermocouples. Figure 6(c) is a photograph for the experimental situation on the roof at 13:20 Feb. 7. The photo shows that Channel 5 is covered with a thick layer of snow. By the influences of the snow layer and the eaves, a V shape snow layer is left on the bottom frame and the channel walls of Channel 4. There is certainly a space between the sheet and the V shape snow for the water falling down. Another snow block formed at the cross of the middle frame and the channel wall between Channels 3 and 4 is still not melted down. Along the left edge of the roof, the adhering snow remains as a shape of half a roll of French bread downstream, and an irregular shape upstream. The photo shows that the weather was shinning then, and the solar radiation was incident upon the falling water film and the accumulated snow. During the experiment, uniform water film flow was observed.

Fig. 6(c). A photograph for the experimental situation on the roof at 13:20 Feb. 7, 1995

4.2 Comparison of Model Predictions with Experimental Data

A typical temperature distribution across the water film thickness is shown in Fig. 7. The data reveal that

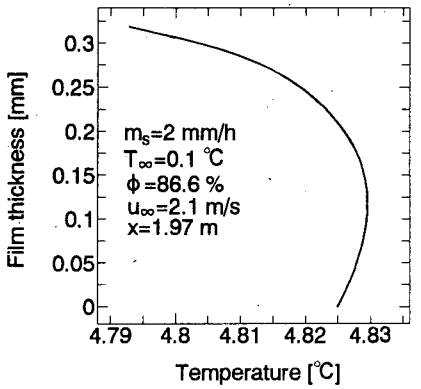

Fig. 7. Typical temperature distrubution aross the water film thickness

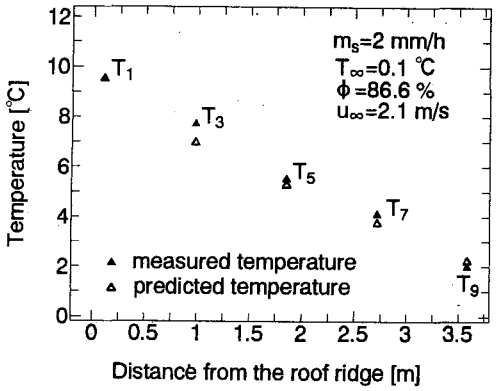

Fig. 8. Comparison of predicted and measured water temperatures in Channel 3 for 18:23 Feb. 6

there is a sharp drop toward the gas-water interface. This is attributed to that latent heat for melting snow and evaporating water at gas-water interface is so large that it causes a marked temperature drop near the interface. The result provides that an increase in heat transfer occurs in a narrow region of about 30 % of the film thickness near the free surface of the water film. The moderate decrease toward the sheet surface should be attributed to the heat transfer across the sheet and wooden roof thickness.

Figure 8 shows the comparison of predicted and measured temperatures in Channel 3 for 18:23 Feb. 6. The predictions agree well with the experimental data. Assuming the same temperatures for the back surface of the wooden roof and the atmosphere makes the calculated values for T_3 and T_7 be smaller than the measured ones. On the other hand, the fixing metal frames on the channel walls above the measuring points of T_5 and T_9 cause T_5 and T_9 to decrease more intensively so that the predicted and measured outlet temperatures, T_9, are in good agreement.

The comparison of predicted and measured outlet water temperatures of Channel 3 for Feb. 6, 1995 is presented in Fig. 9. Corresponding to the average values for the weather condition such as snowfall intensity, wind speed and relative humidity, the measured outlet temperature for each of the 24 hours in Fig. 9 was obtained by utilizing the average of two scanned temperature drops between T_1 and T_9 in every hour. The predictions are in good agreement with the measured temperatures. The data reveal that the predicted values is higher than the measured ones as the atmospheric temperature drops to below 0 ℃, and lower than the experimental values for a higher atmospheric temperature. These can be attributed to the influences of the metal channel walls and the fixing metal frames. The atmosphere around the channel walls and the fixing frames generally is at the saturation state. As the atmospheric temperature drops to below 0

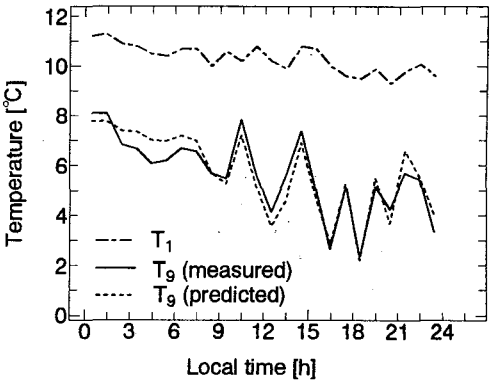

Fig. 9. Comparison of predicted and measured outlet water temperatures of Channel 3 for Feb. 6, 1995

℃, frost might adhere to the frames and the walls, which needs much heat to melt it. Therefore the water temperature drops more. During the day time, the higher atmospheric temperature reduces the temperature drops caused by the heat transfer through the channel walls and the fixing frames. Moreover a small magnitude of diffuse solar radiation contributes to reducing the water temperature drop. The other factors such as unsteady weather condition and actual three dimensional heat transfer also influence the deviation between the predicted and measured temperatures.

5. CONCLUSIONS

The experiment was performed for melting falling snow on roofs using warm water flowing along sheet channels in Tookamachi city, Nigata prefecture from February 6 to February 7, 1995. The sheet surface temperatures at 11 positions in 3 channels were measured. The performance of the present system was examined under snow weather condition. A fully spread uniform water film in the sheet channel was observed. The experimental results revealed that it was feasible to use warm water flowing along sheet channels for melting falling snow on roofs. The temperature drop in the sheet channel mainly depended on the snowfall intensity, atmospheric temperature and wind speed. By the influence of the roof edge, the temperature drop in Channel 1 was much larger than that in Channel 3. A water-snow two phase flow or a snow covered frozen water was experienced temporarily in the lower reach of the water flowing channel. These suggest that a larger water flow rate is needed for the channel next to the side edge, and a higher inlet temperature or a greater water flow rate is required for a severe weather condition, under which the continuous heavy snow falls and the atmospheric temperature is at several degree blow 0 Celsius. There was reasonably good agreement between the measured and predicted water temperatures.

ACKNOWLEDGEMENTS

The first author is a visiting scholar from the People's Republic of China. He is grateful to the China Flight Test Establishment (Xi'an, China) for supporting him during the course of this study.

REFERENCES

(1) V. G. Lunardini: Heat Transfer in Cold Climates, Van Nostrand Reinhold Company (1981).

(2) S. Fukusako and H. Inaba: Heat Transfer Phenomena in Low Temperature Environment and Their Applications, Yokendo Ltd. (1996) (in Japanese).

(3) T. Tsukidate, H. Hoshina, K. Shibata, T. Tashiro, M. Kimura and H. Yokoyama: Trans. Of the Society of Heating, Air-conditioning and Sanitary Engineers of Japan, No. 68, (1998), 55 (in Japanese).

(4) S. V. Patankar: Numerical Heat Transfer and Fluid Flow, Hemisphere/McGraw-Hill, (1980).

(5) T. Yamazaki: Snow and Ice, 60, (1998), 131 (in Japanese).

(6) Japanese Society of Mechanical Engineers (ed.): Measurements of Humidity and Water Content as well as Monitor of Environment, Gihodo Press Ltd. (1992) (in Japanese).